

Supplementary Information

Channel Function of Polycystin-2 in Endoplasmic Reticulum Protects Against Polycystic Kidney Disease

Biswajit Padhy^{1,3}, Jian Xie^{1,3}, Runping Wang¹, Fang Lin², and Chou-Long Huang^{1,*}

¹Department of Medicine, Division of Nephrology and ²Department of Anatomy and Cell Biology,
University of Iowa Carver College of Medicine, Iowa City, Iowa, USA

Index:

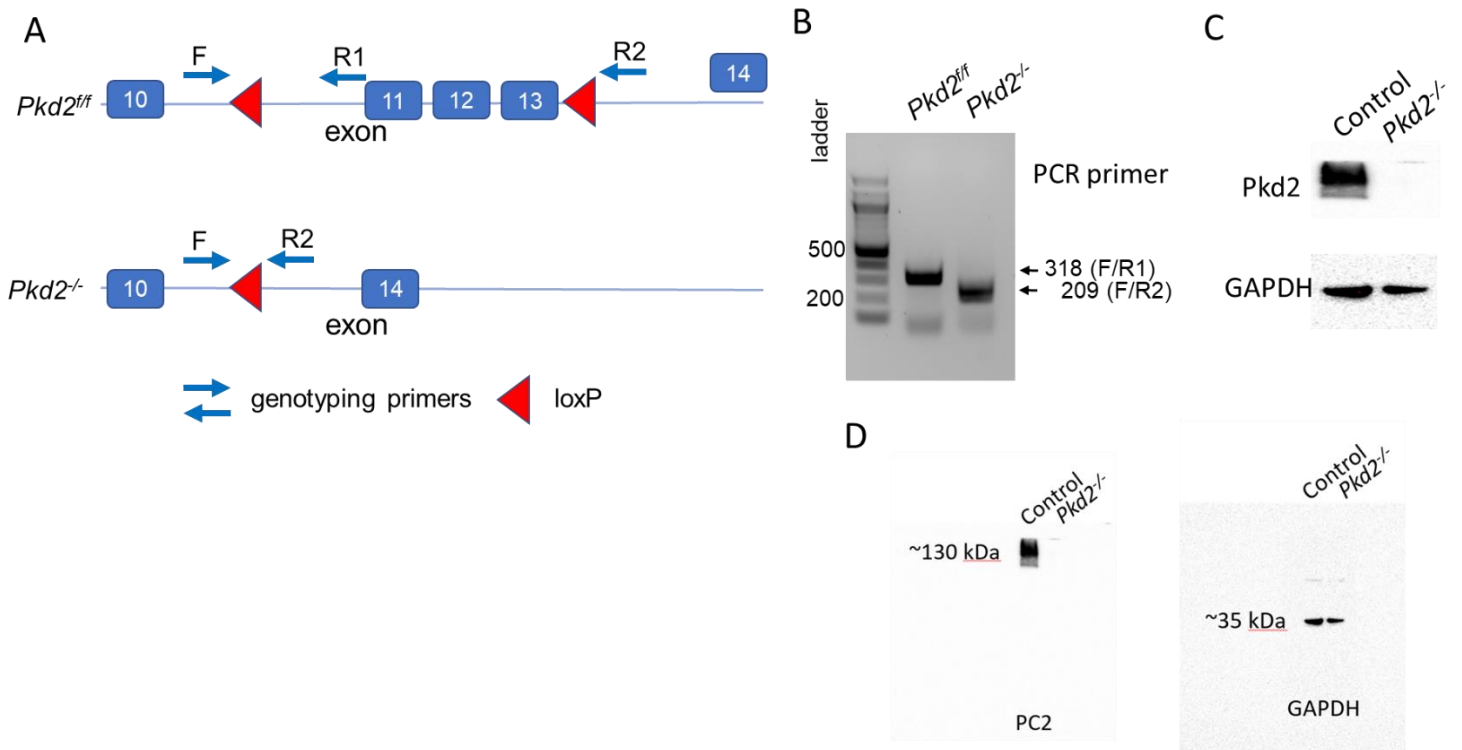
Supplementary Table 1

Supplementary Figure 1-15

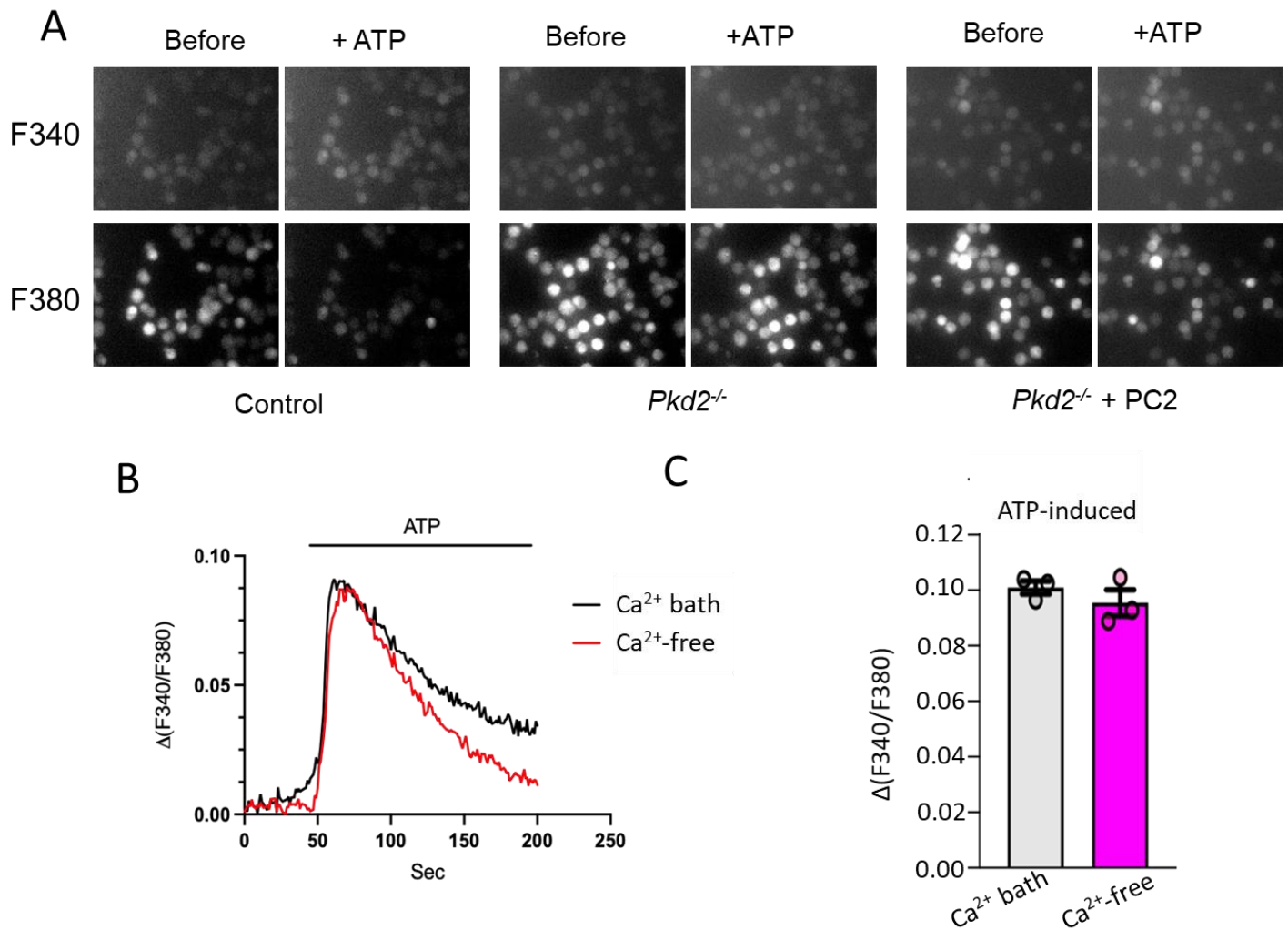
Supplementary Table 1. Distribution of pups from breeding between *TricB*^{+/-} parents.

<i>TricB</i> ^{+/+} (25%)	<i>TricB</i> ^{+/-} (50%)	<i>TricB</i> ^{-/-} (25%)	Total
8/ [42%]	11/ [58%]	0	19

Genotyping was performed on pups ~P5. Total 19 pups from multiple rounds of breeding were genotyped. The frequency of genotypes predicted from mendelian distribution and actual frequency are shown in parentheses and bracket, respectively.



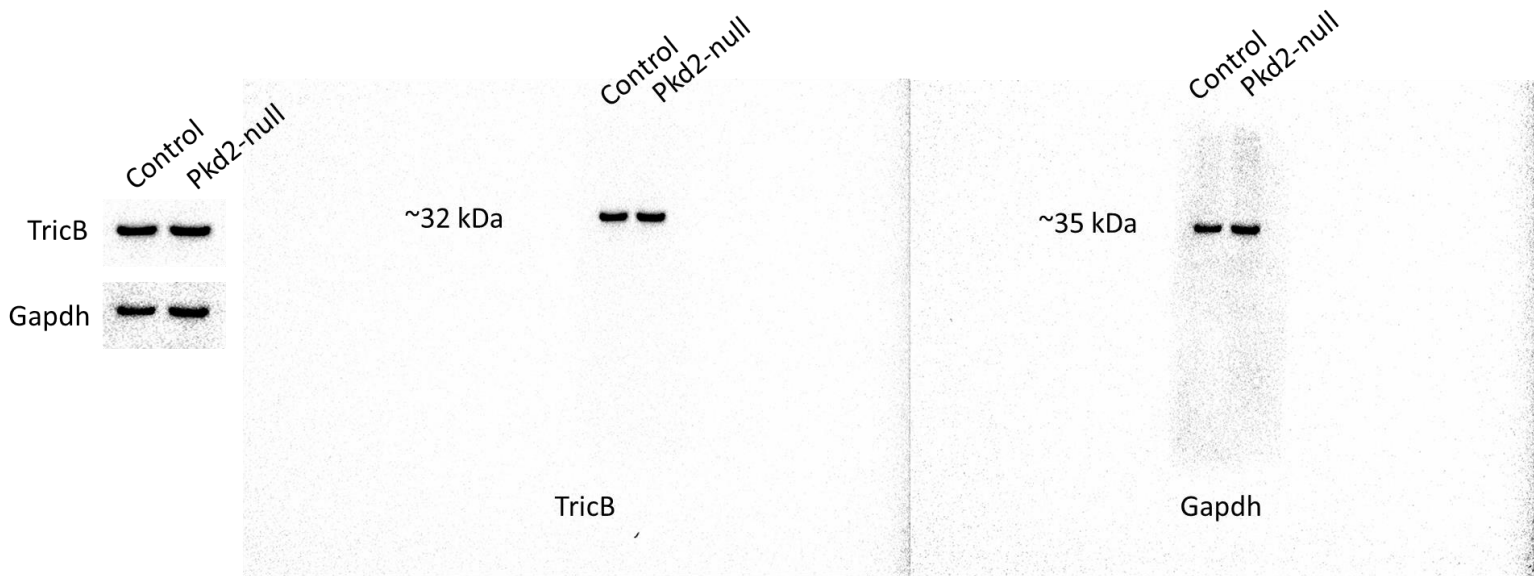
Supplementary Figure 1. Generation of *Pkd2*-null renal epithelial cell line. (A) Diagram depicting partial mouse *Pkd2* genome and location of forward (F) and two reserve (R1 and R2) primers (5' to 3'; CCTTTCCTCTGTGTTCTGGGGAG, GTTTGATGCTTAGCAGATGATGGC, CTGACAGGCACCTACAGAACAGTG, respectively) in relation to exons of *Pkd2* and *loxP* sites. Primers F and R1 amplify a 318 bp product in the floxed allele while deletion of floxed region by Cre-recombinase yields a 209 bp product from primers F and R2 for the *Pkd2*-null allele. (B) Gel picture showing genotype of *Pkd2^{fl/fl}* and *Pkd2*-null cells. Genotyping PCR was performed with F, R1, and R2 primers included in the same reaction mixture. (C) Western blot analysis validating loss of PC2 in *Pkd2^{-/-}* cells. (D) Uncut full-length western blot gel used in panel C.



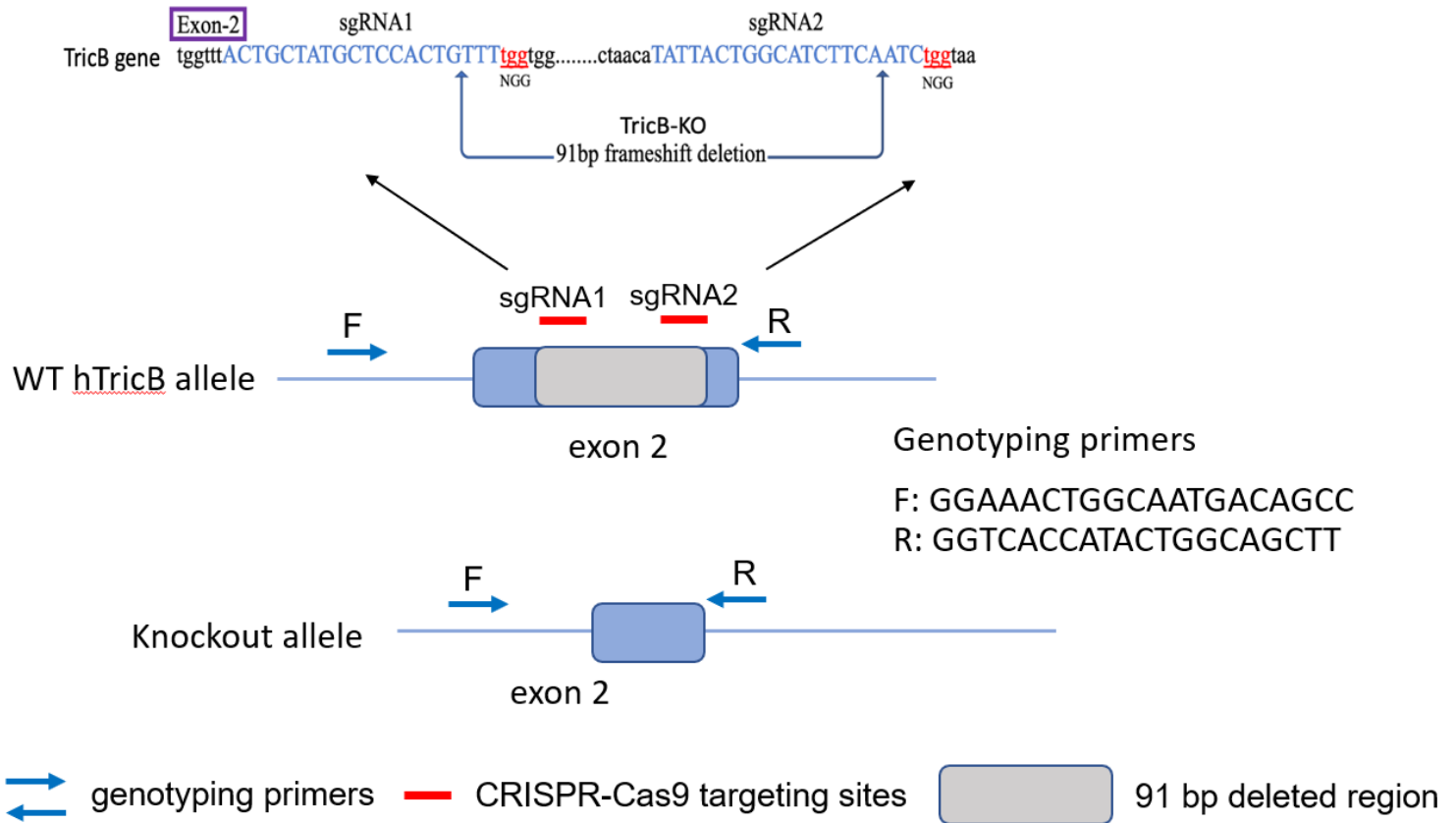
Supplementary Figure 2. Loss of PC2 underlies intracellular Ca²⁺ release defect in *Pkd2*-null cells. (A) Representative pictures showing cells loaded with Fura2-AM before and after stimulation with 100 μ M ATP for control, *Pkd2*^{-/-} and PC2-overexpressed *Pkd2*^{-/-} cells. Upper panel of pictures are images of fluorescence at 340 nm excitation (F340) while lower panel at 380 nm excitation (F380). (B) Representative baseline normalized ATP-induced [Ca²⁺]_i transients (above the baseline level) in control (wildtype) epithelial cells in Ca²⁺-containing (black trace) and Ca²⁺-free bath (red trace). Shown are increases in the ratio of emission fluorescence at excitation wavelength 340 nm over 380 nm [$\Delta(F340/F380)$]. Total 6 separate experiments were conducted, 3 in the presence of 1.2 mM Ca²⁺ bath, and 3 in Ca²⁺-free bath. Each experiment (trace) contains the average of 3 individual cover slips with multiple cells on each cover slip. The results show that peak Ca²⁺ transients (reflecting ER Ca²⁺ release) are not different, but the second phase (likely from Ca²⁺ influx) is higher in Ca²⁺-containing bath. (C) Means \pm SEM of results (peak $\Delta(F340/F380)$ values) from 3 experiments for Ca²⁺-containing and Ca²⁺-free bath as in Panel B.

Main Figure 1G

Un-cut full western blot for Main Figure 1G

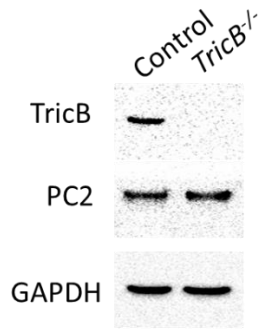


Supplementary Figure 3. Un-cut full western blot for main Figure 1G.

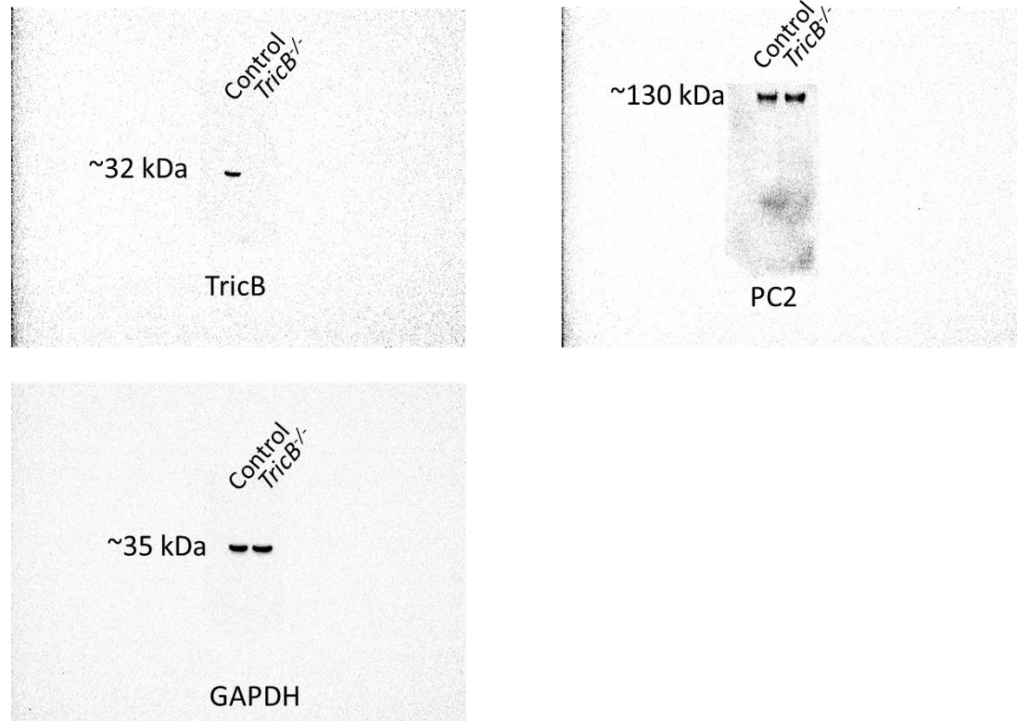


Supplementary Figure 4. Diagrammatic presentation shows location of sgRNA1 and sgRNA2 targeting exon-2 of wild-type human *TRICB* allele. Through CRISPR-cas9 both sgRNAs are used to introduce a 91 bp frameshift deletion within exon-2. Indicated are forward (F) and reverse (R) primer surrounding the targeted region used for genotyping both WT (443 bp) and knockout allele (352 bp) (Figure 2A).

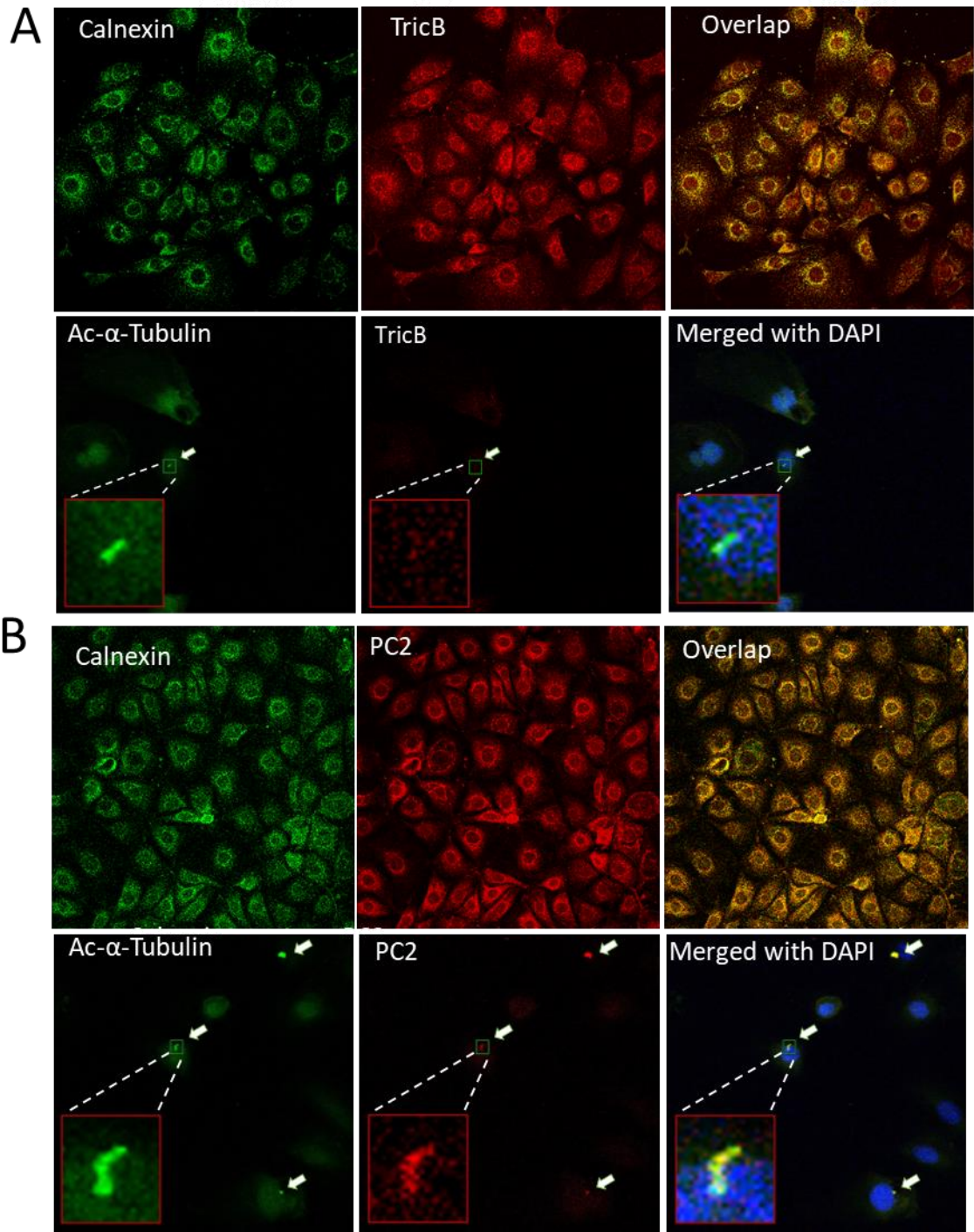
Main Figure 2B



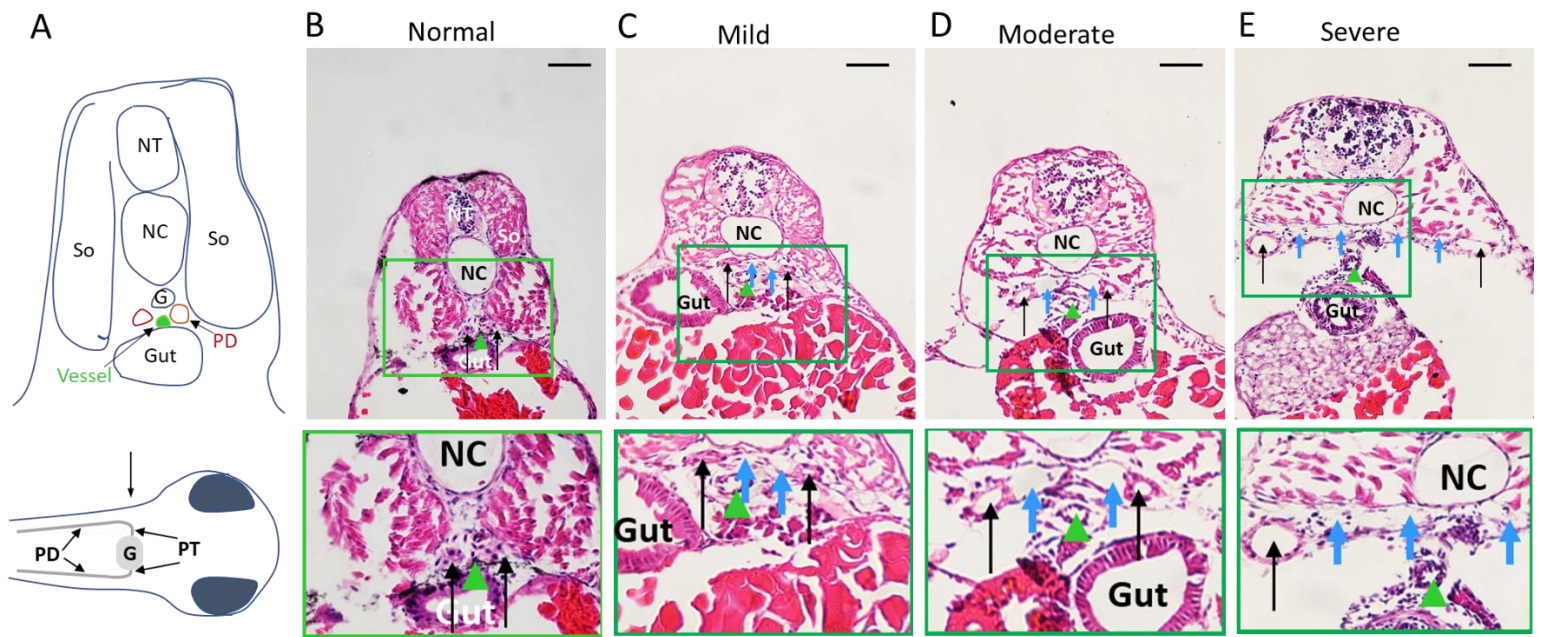
Un-cut full western blot for Main Figure 2B



Supplementary Figure 5. Un-cut full western blot for main Figure 2B.



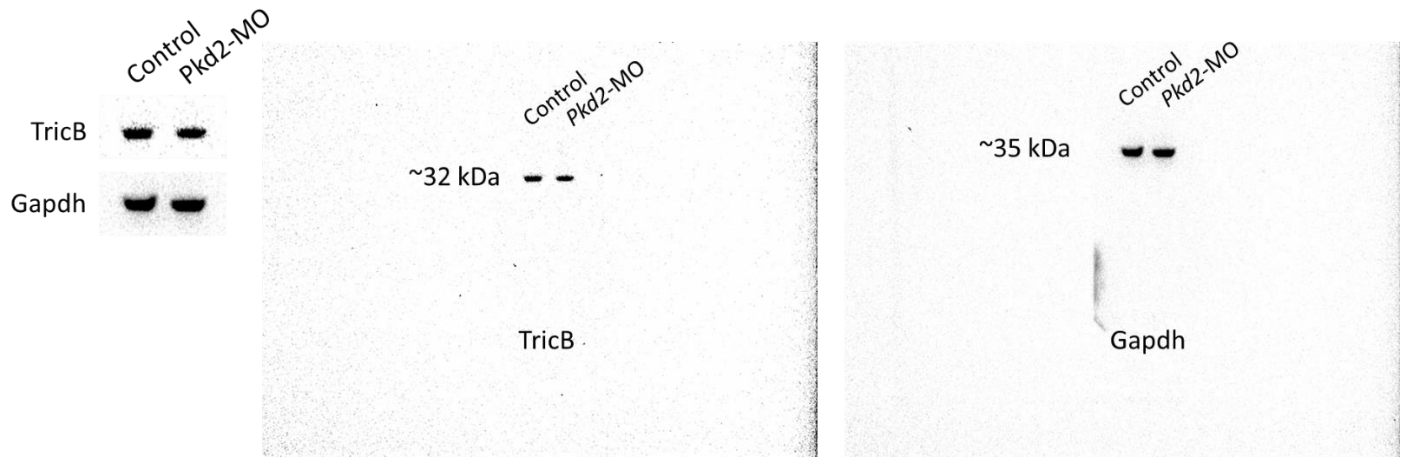
Supplementary Figure 6. TricB is localized to ER, but not the primary cilium. (A) Top: Double immunofluorescent imaging by con-focal microscopy in renal epithelial cells shows localization of endogenous TricB overlaps with the ER marker calnexin surrounding the nuclei stained with DAPI. Imaging obtained by 20X objective. Bottom: Absence of TricB in the primary cilium marked by staining for acetylated α -tubulin. Imaging obtained by 63X objective. (B) Top: Colocalization of endogenous Pkd2 overlapping with the ER marker calnexin in renal epithelial cells. Imaging obtained by confocal microscopy with a 20X objective. Bottom: Presence of PC2 in the cilium marked by staining for acetylated α -tubulin. Imaging obtained by 63X objective.



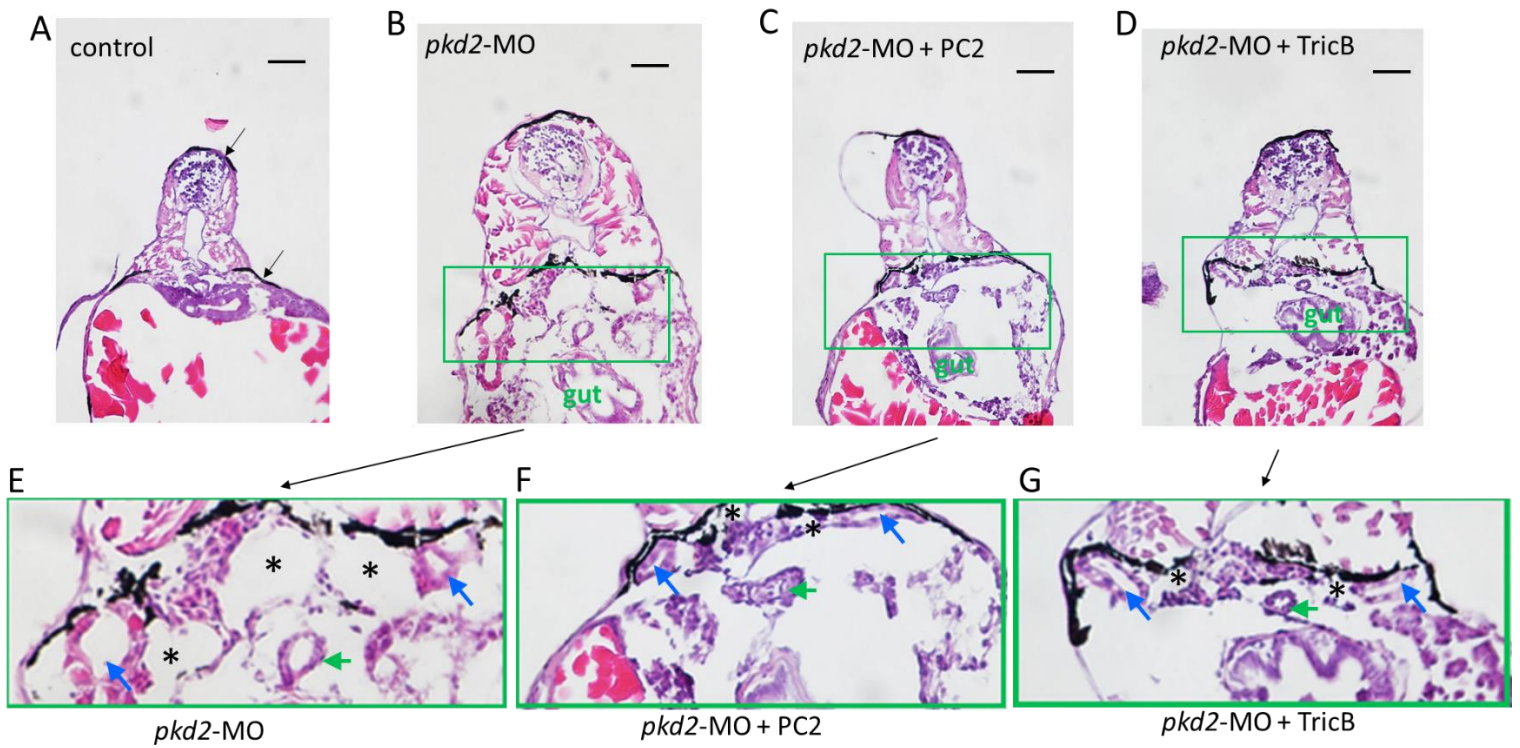
Supplementary Figure 7. Correlation between tail curvature and pronephric cyst formation (i.e., pronephric tubular cyst and pronephric duct dilatation). (A) Diagrammatic presentation showing the structure of pronephros in zebrafish embryo. Upper panel corresponds to the transverse section while lower panel to the longitudinal section of the zebrafish larvae. Glomerulus (G), pronephric tubules (PT), pronephric ducts (PD), somites (So), notochord (NC) and neural tube (NT). (B-E) H&E staining of cross-sections of zebrafish embryos at ~3 dpf showing a pair of pronephric ducts connected to centrally fused glomerulus through pronephric tubules in the control embryos. (B) and *pkd2*-MO injected embryos grouped into mild (C), moderate (D) and severe (E) based on tail curvature. Pronephric duct (black arrow), pronephric tubular cyst (blue thick arrow) and vessel (green arrowhead). Scale bars: 50 μ m.

Main Figure 3B

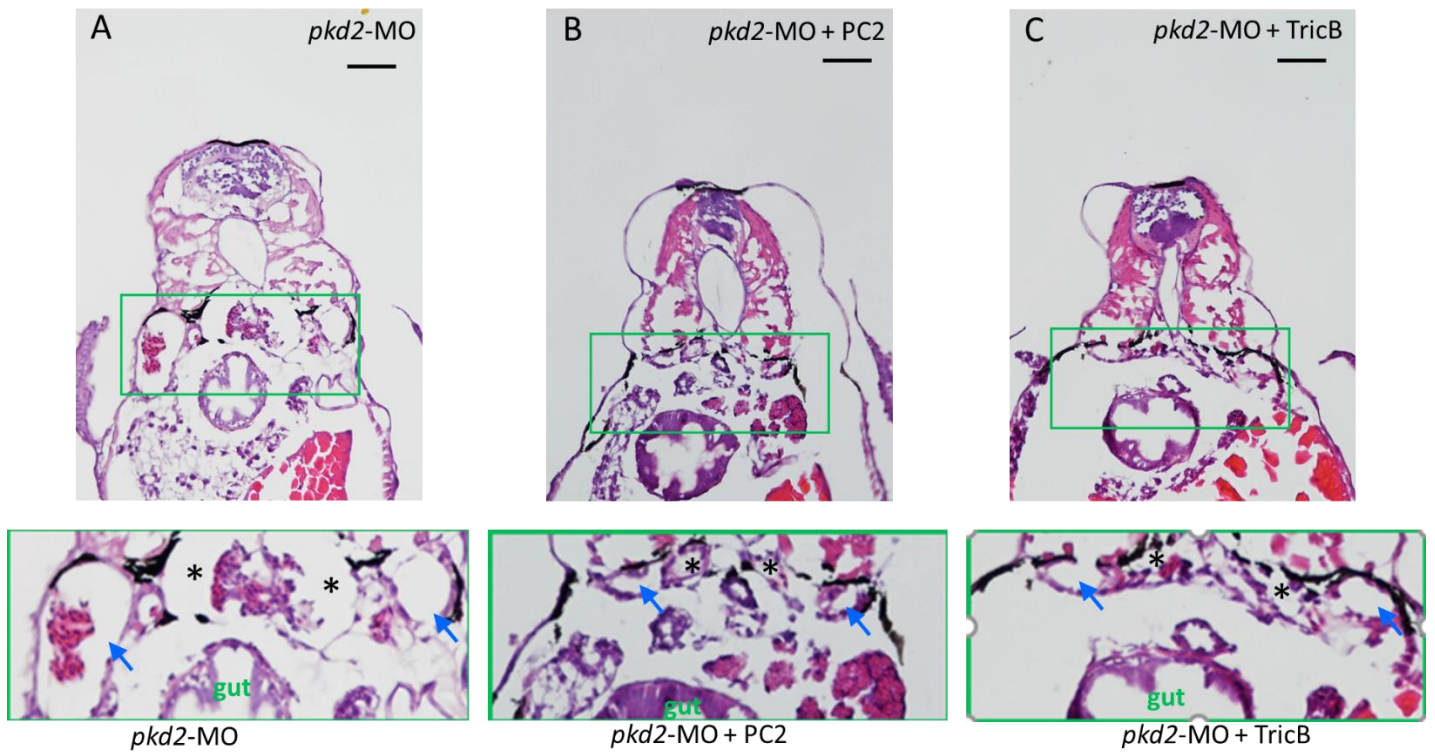
Un-cut full western blot for Main Figure 3B



Supplementary Figure 8. Un-cut full western blot for main Figure 3B.

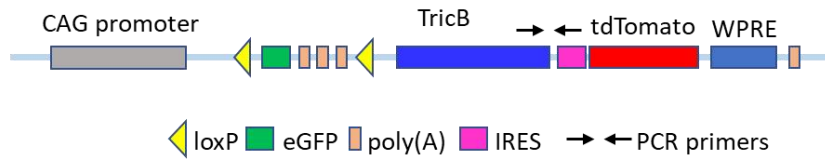


Supplementary Figure 9. Co-injecting with *Pkd2* mRNA (encoding PC2) or with *TricB* in *pkd2*-MO embryos suppresses pronephric cyst formation (pronephric duct dilatation and pronephric cyst). Upper panels (A-D) H&E staining of cross-sections of zebrafish embryos showing the structure of pronephros in the control (A) and *pkd2*-MO injected with *pkd2* morpholino with along with vehicle (B), mRNA for mouse *Pkd2* (C) or *TricB* (D). Lower panels (E-G) are the enlarged images of corresponding green boxes. Pronephric duct (blue arrows), pronephric tubular cysts (asterisk) and vessel (green arrows) Thin arrows in panel A indicates pigment lines. Scale bars: 50 μ m.

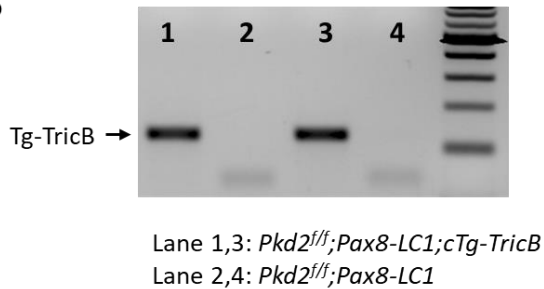


Supplementary Figure 10. Additional examples showing co-injecting with *Pkd2* (encoding PC2) or with TricB in *pkd2*-MO embryos suppresses pronephric duct dilatation and pronephric tubular cyst formation. Upper panels (A-D) are H&E staining of cross-sections of zebrafish embryos showing the structure of pronephros in *pkd2*-MO injected with *pkd2* morpholino (A) and along with mRNA for mouse *Pkd2* encoding PC2 (B) or TricB (C). Lower panels are the enlarged images of corresponding green boxes. Pronephric duct (blue arrow), pronephric tubular cysts (asterisk). Scale bars: 50 μ m.

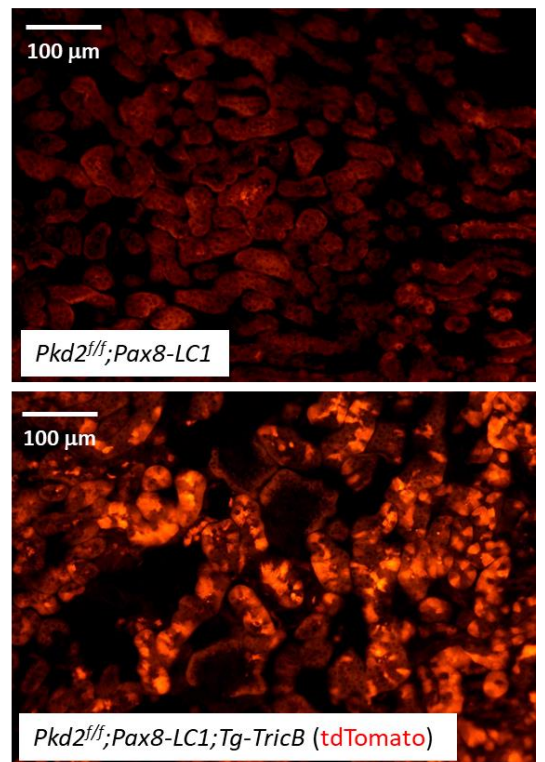
A



B

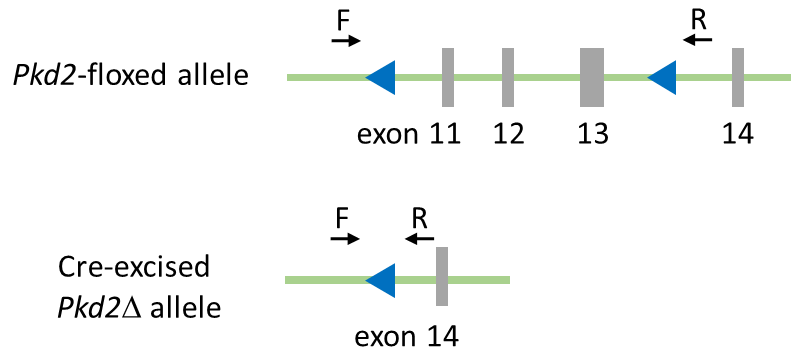


C

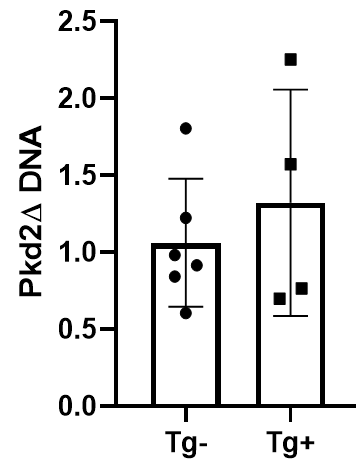


Supplementary Figure 11. Transgenic *TricB* expression in the kidneys of *cTg-TricB* mice. (A) *cTg-TricB* transgene construct. The transgene is driven by CAG promoter, followed by a floxed eGFP-triple poly(A) cassette, mouse *TricB* cDNA, and IRES-tdTomato reporter elements. *TricB* and tdTomato are expressed in Cre active cells where the poly(A) cassette is excised. (B) Detection of *TricB* transgene mRNA by RT-PCR in kidneys of *cTg-TricB*⁺, *Cre*⁺ mice (lane 1,3), but not in mice without the transgene (lane 2,4). Primers: F, 5'-ACCGTCTTCCAATGGTTCTG; R, 5'-CGCTCTAGAACTAGCATGGC. It is transgene-specific since the reverse primer targets the vector sequence downstream of *TricB* cDNA. (C) Transgene expression confirmed by tdTomato signals in the kidneys of *cTg-TricB*-positive, *Cre*⁺ mice, as compared to *Tg-TricB*-negative control kidney.

A



B

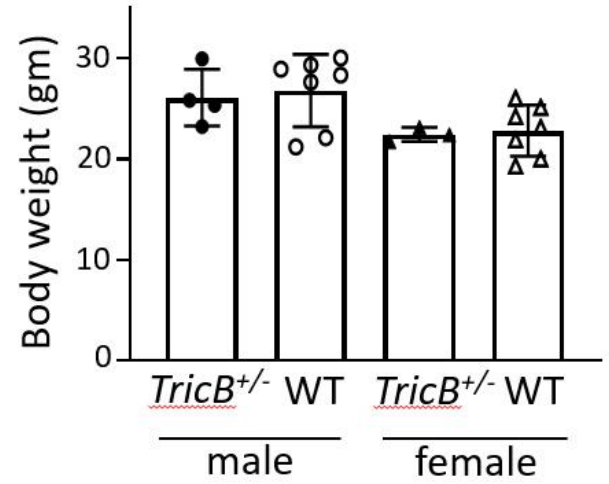


Supplementary Figure 12. Detection of *Pkd2* knockout allele in the kidneys of *Pkd2*-cKO mice with and without *Tg-TricB*. (A) Primers flanking the two *loxP* sites only detect excised *Pkd2* allele under the condition of PCR reaction. Forward (F) and reverse (R) primers: 5'-CCT TTC CTC TGT GTT CTG GGG AG; 5'-CTG ACA GGC ACC TAC AGA ACA GTG). (B) Quantitative PCR of kidney genomic DNA shows that *Pkd2*-cKO mice with and without *Tg-TricB* have no difference in the levels of *Pkd2* knockout allele (“*Pkd2* Δ ”) in kidney.

A

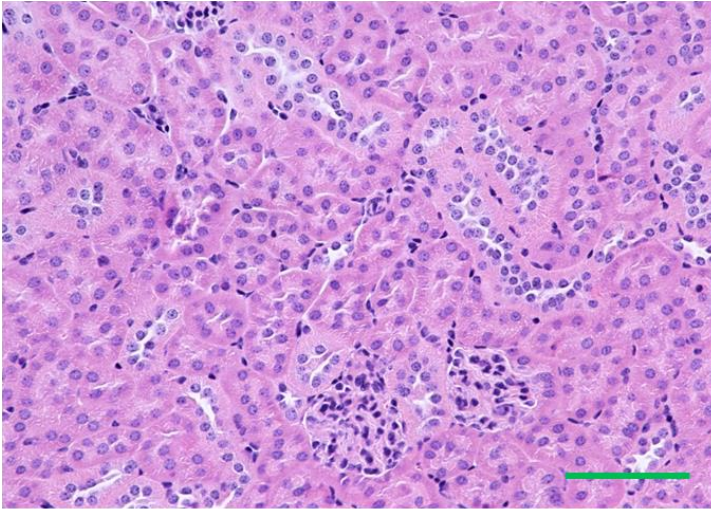


B

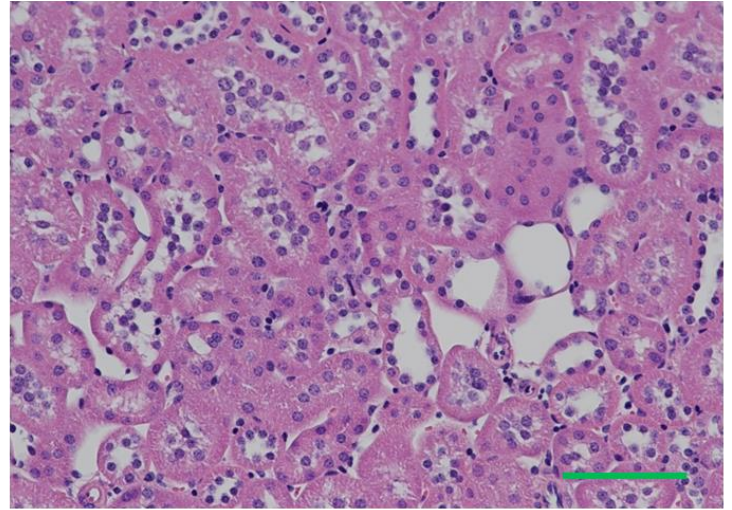


Supplementary Figure 13. Mice heterozygous for *TricB* are grossly normal. (A) *TricB*^{+/-} mice have grossly normal appearance and body weight compared to wild type littermates at ~3 months. (B) Body weight of *TricB*^{+/-} and wild type littermates at ~3 months.

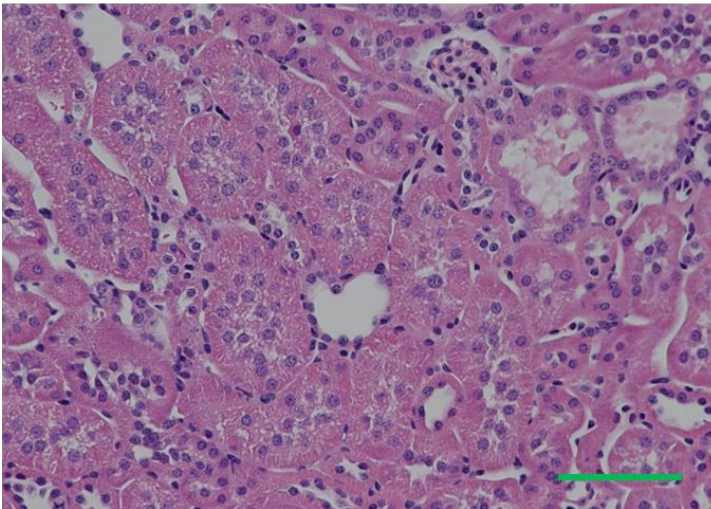
A *Pkd2^{f/+};Ksp-Cre* (KW/BW ~0.8%)



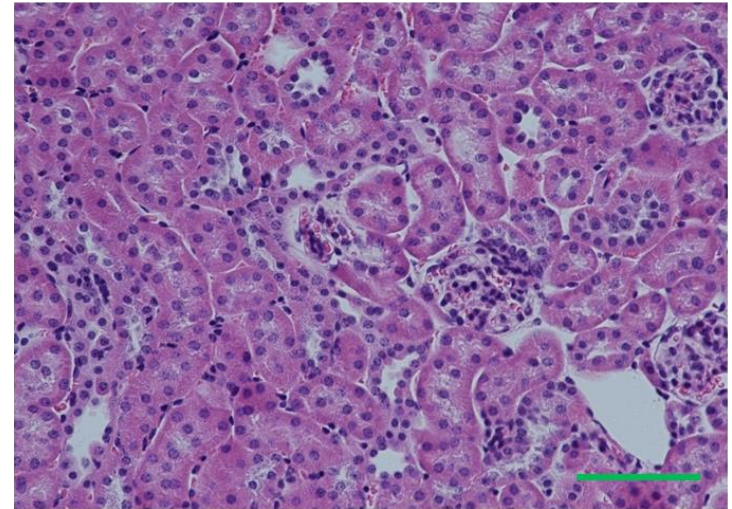
B *Pkd2^{f/f};Pax8-LC1* (KW/BW ~2%)



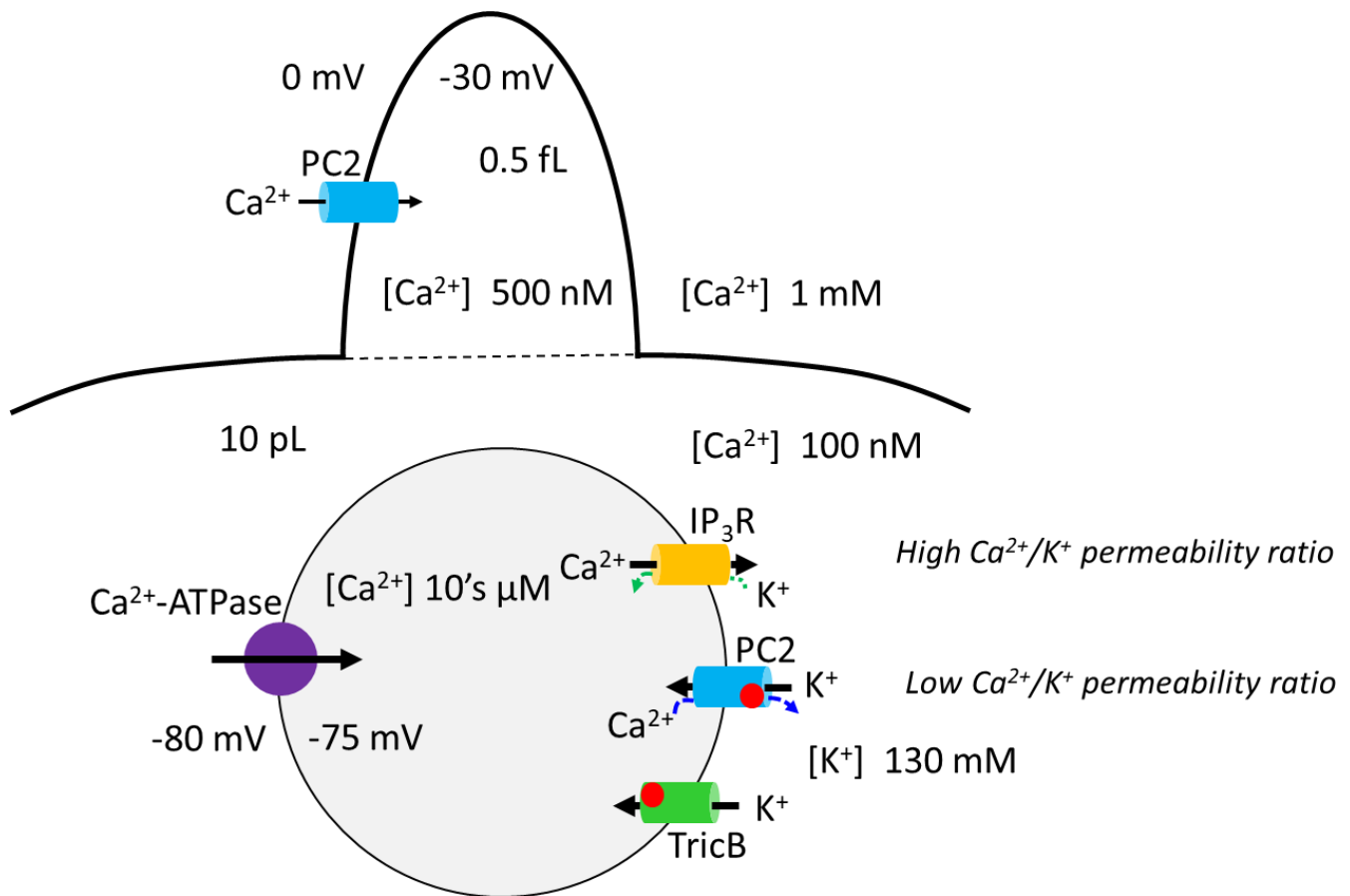
C *Pkd2^{f/+};TricB^{f/f};Ksp-Cre* (KW/BW ~1.1%)



D *Pkd2^{f/+};TricB^{f/f};Ksp-Cre* (KW/BW ~1.1%)



Supplementary Figure 14. Cyst formation in *Pkd2^{f/+};TricB^{f/f};Ksp-Cre* mouse kidneys is comparable to early-stage cyst growth in doxycycline-induced *Pkd2*-deleted adult kidney. H&E stained kidney sections of *Pkd2^{f/+};Ksp-Cre* mice (A), *Pkd2^{f/f};Pax8-LC1* mice (B), and *Pkd2^{f/+};TricB^{f/f};Ksp-Cre* mice (C, D). *Pkd2^{f/+};Ksp-Cre* and *Pkd2^{f/+};TricB^{f/f};Ksp-Cre* mice are ~6 month old with KW/BW ratio ~0.8% (within the range of control) and ~1.1%, respectively. The ~1.1% KW/BW ratio in *TricB^{f/f};Ksp-Cre* mice is significant higher than ~0.8% in *Pkd2^{f/+};Ksp-Cre* ($p = 0.002$). See main Figure 8 and associated text for further details and information. Kidney section in panel B is from a 6 weeks old *Pkd2^{f/f};Pax8-LC1* mice induced by doxycycline for 2.5 months with KW/BW ~2%. Scale bar is 50 μm .



Supplementary Figure 15. Working model illustrating PC2 as an ER K⁺ channel. The intraciliary volume is 0.5 fL versus cytosol ~10 pL. Ca²⁺ is actively transported into ER by Ca²⁺-ATPase to maintain ER luminal [Ca²⁺] at ~10's μM and ~5 mV lumen-positive potential across ER membrane (absolute potential -75 mV relative to extracellular). The concentration and electrical gradient for Ca²⁺ movement are 2,000-fold (1 mM to 500 nM) and -30 mV for ciliary membrane versus 100-fold (10 μM to 100 nM) and -5 mV for ER membrane, respectively. Ca²⁺/K⁺ permeability ratio for PC2 is much lower than for IP₃R (see text for details). Thus, while PC2 also conducts Ca²⁺ (illustrated by thin blue dotted line) it may not be an efficient Ca²⁺ release channel versus IP₃R (see note below). Ca²⁺ efflux through IP₃R leaves behind negative charges in ER lumen to impede further Ca²⁺ efflux. The cytosolic [K⁺] is ~130 mM. K⁺ influx through TricB and ER-resident PC2 will facilitate ER Ca²⁺ release. Cl⁻ efflux in parallel with Ca²⁺ efflux may also play a role in some cells (not shown). Note that it has been suggested that IP₃R may conduct small K⁺ influx to function as its own Ca²⁺-K⁺ exchanger (thin green dotted line). Red dot in the ER luminal side of TricB and intracellular side of PC2 indicates sites for Ca²⁺ binding and regulation. Different regulatory mechanisms underscore needs for both TricB and PC2 and their synergism. Note: While Ca²⁺ efflux directly through ER-localized PC2 is unlikely to impact cytosolic [Ca²⁺] globally, local cytosolic [Ca²⁺] may be sufficiently elevated to exert physiological importance. PC2 is also reported present on the plasma membrane, though much lower abundance than in ER. The potential role of plasma membrane PC2 in Ca²⁺ homeostasis is not illustrated here.